◆ Human Brain Mapping 6:383–389(1998) ◆

ERP and fMRI Measures of Visual Spatial Selective Attention

George R. Mangun,[1]* Michael H. Buonocore,[2] Massimo Girelli,[1,3] and Amishi P. Jha[1]

[1]*Department of Psychology and Center for Neuroscience, University of California, Davis, California*
[2]*Department of Radiology, University of California, Davis, California*
[3]*Department of Visual Science, University of Verona, Italy*

Abstract: In two prior studies, we investigated the neural mechanisms of spatial attention using a combined event-related potential (ERP) and positron emission tomography (PET) approach (Heinze et al. [1994]: Nature 392:543–546; Mangun et al. [1997]: Hum Brain Mapp 5:273–279). Neural activations in extrastriate cortex were observed in the PET measures for attended stimuli, and these effects were related to attentional modulations in the ERPs at specific latencies. The present study used functional magnetic resonance imaging (fMRI) and ERPs in single subjects to investigate the intersubject variability in extrastriate spatial attention effects, and to qualitatively compare this to variations in ERP attention effects. Activations in single subjects replicated our prior group-averaged PET findings, showing attention-related increases in blood flow in the posterior fusiform and middle occipital gyri in the hemisphere contralateral to attended visual stimuli. All subjects showed attentional modulations of the occipital P1 component of the ERPs. These findings in single subjects demonstrate the consistency of extrastriate attention effects, and provide information about the feasibility of this approach for integration of electrical and functional imaging data. *Hum. Brain Mapping 6:383–389, 1998.* © 1998 Wiley-Liss, Inc.

Key words: ERP; fMRI; spatial attention; visual stimuli

INTRODUCTION

Attending and ignoring events in the visual world significantly influences how they are processed and perceived. Electrophysiological investigations in animals [e.g., Moran and Desimone, 1985; Motter, 1994], and in humans [e.g., Eason et al., 1969; Van Voorhis and Hillyard, 1977; see Mangun, 1995 for a review] have demonstrated that sensory-evoked visual activity is modulated by selective attention. In humans, functional neuroimaging has also been utilized successfully to identify the anatomical loci of attentional modulations in stimulus processing, and has demonstrated that selective attention can influence visual input analysis in discrete regions of extrastriate visual cortex [e.g., Corbetta et al., 1991; Heinze et al., 1994; Mangun et al., 1997; Woldorff et al., 1997].

We investigated the relationship between electrophysiological and functional imaging measures of selective attention in recent studies of spatial selective attention in humans [Heinze et al., 1994; Mangun et al., 1997]. Electromagnetic (EEG and MEG) and functional neuroimaging (PET and fMRI) measures provide complementary views of brain function, each emphasizing slightly different aspects of information process-

*Correspondence to: Dr. George R. Mangun, Center for Neuroscience, University of California, Davis, CA 95616. E-mail: grmangun@ucdavis.edu

Received for publication 20 February 1998; accepted 8 July 1998

ing in the nervous system. Event-related potentials (ERPs) recorded from the scalp or intracranially, provide direct, high-temporal resolution signatures of neural activity. In contrast, functional imaging methods yield high-anatomical resolution measures of the blood flow that is coupled to neuronal activity [see Mangun et al., 1998a for a theoretical discussion]. In our above referenced studies, we found that visual selective attention to stimuli in one visual half-field resulted in increases of regional cerebral blood flow (rCBF) in the posterior fusiform and middle occipital gyri of the hemisphere contralateral to the attended hemifield. Based on modeling of electrical activity, and observed covariations in attention effects for ERPs and rCBF, we proposed that a well-established ERP spatial attention effect, known as the P1 effect (80–130 msec poststimulus latency), was most likely generated in the posterior fusiform gyrus in human extrastriate visual cortex. This was significant because the P1 attention effect in the visual ERPs is the earliest electrical sign of selective attention to be consistently observed in humans in visual tasks [e.g., Luck et al., 1994; Mangun et al., 1993].

In the present study, the goal was to replicate our previous findings in PET using fMRI in order to more closely relate the attentional activations to individual cortical anatomy. In addition, we wished to assess the degree of variability of extrastriate cortical attention effects across subjects, and especially, to determine whether all subjects who showed modulations in the posterior fusiform gyrus also showed middle occipital activations. Similarly, this study permitted us to determine whether all subjects who showed clear P1 attention effects in the ERPs, also showed consistent modulation of the posterior fusiform gyrus, and vice versa. The design was similar to the paradigm we have used previously except that the attention conditions were now varied between attend-left and attend-right every 16 sec during a run of 4 min 48 sec duration—in the prior PET studies the attention conditions were blocked over 2 min periods and were separated by about 10 min between scans.

METHODS

Design

Stimuli consisted of bilateral arrays of four symbols (approximately 2.0 × 1.0 degrees of visual angle each) flashed in rapid (ISI = 250–550 msec) sequence on a translucent back-projection screen under computer control. The subjects were reclined in the scanner and wore prism glasses to view the stimuli on the screen that was positioned near their feet. The symbols were in the upper visual field (approximately 1.0 degree from the horizontal meridian to bottom edge) and were located at eccentricities of approximately 4.0 and 5.5 degrees (to center of symbol) in the left and right visual half fields. Stimulus durations were 50 msec, and the symbols were presented in white on a black background. There was a central fixation square and two outline boxes present continuously on the screen throughout the sequence—the boxes demarcated the stimulus locations.

Subjects (n = 6) were healthy volunteers with normal vision and were all right-handed. A custom built bite bar minimized head movements in the scanner. They were instructed to fixate a central square on the screen and maintain fixation. A warning stimulus indicated the beginning of a 32 sec baseline period where scans were taken and the background and fixation point display was visible but no task was being performed. At the end of the 32 sec baseline, an arrow appeared at fixation that indicated which hemifield to attend (covertly) for the next 16 sec; the arrow remained on the screen for the duration of each 16 sec epoch. The subjects were admonished to maintain eye position on the center of the fixation point. Prior to the fMRI session, an ERP session permitted training of the subjects in the task and in maintaining fixation, and those who could not maintain fixation in this session, as indicated by electrooculographic recordings and infrared video camera monitoring, were not invited to participate in the fMRI session. The subjects were all graduate students or postdoctoral researchers with high motivation to comply with the experimental instructions, and were experienced observers. The direction of the arrow, and hence direction of attention alternated every 16 sec for the remainder of the 4 min 48 sec run. A random 10% of the arrays contained targets consisting of identical symbols in one hemifield; these required a manual right-hand button press by the subjects when the targets appeared at the attended location. The subjects were explicitly told to ignore the stimuli in the opposite field, which was the preferred strategy in order to detect the targets in the attended hemifield.

Scanning and analyses

Functional images were obtained using a General Electric (GE) Signa 1.5 Tesla whole-body scanner with an elliptical end-capped quadrature radio frequency and local gradient head coil (Medical Advances, Inc.) designed for whole-brain volume echo planar imaging (EPI). EPI images were obtained using gradient re-

called echo in the coronal plane. Sixteen separate interleaved slices were collected with a 2.0 sec repetition time (TR), and a time to echo (TE) of 40 ms, and flip angle (FA) of 90 degrees. Slice thickness was 6 mm with an interslice gap of 2 mm, allowing whole-brain volume imaging beginning with the occipital pole and ending posterior to the frontal pole. However, for the purposes of the present report, we only considered the data from those two slices that corresponded to the region of visual cortex where our prior PET studies revealed significant activations. A 64 × 64 matrix and 22 cm field of view (FOV) was used, yielding an effective voxel size of 3.43 mm × 3.43 mm × 6 mm. Fourier image reconstruction included the application of N/2 ghost correction using image phase correction [Buonocore and Gao, 1997]. Neural activation was detected by the blood oxygenation level dependent (BOLD) contrast mechanism [e.g., Kwong et al., 1992; Ogawa et al., 1992] that lead to differences in magnetization using T2* weighted EPI. High-resolution proton density fast spin echo images (512 × 512 matrix, 22 cm FOV) were also obtained in the coronal plane during the same scanning session to provide anatomical images for coregistration with the functional images. These anatomical scans were acquired with the following parameters: TR = 4.2 sec; TE = 36 and 136 ms; echo train = 8; 6 mm skip 2 mm slices.

High pass filtering, using a 16-image moving average, was applied at each pixel to remove low frequency temporal drifts of the signal. Functional activation was assessed by linear vector space analysis [Bandettini et al., 1993]. Task specific functional activation was assessed by computing the linear correlation coefficient (*r*) of these signal changes with a box-car reference waveform that represents the periodic alterations in the experimental conditions (e.g., attend-left vs. attend-right, etc.). Statistical significance was determined after computing the corrected degrees of freedom (*df*). This was done by comparing the strength of activation of allegedly activated pixels (using *r*) with the distribution of strength of unactivated pixels in the brain image. The histogram of *r* values from a sample population of unactivated pixels (i.e., the central *r* distribution in the whole brain) was used to derive the corrected *df*. An estimation of the *df* is necessary because the noise in the time series cannot be assumed to be white noise, due to the presence of correlated physiological noise [Buonocore and Maddock, 1997; c.f., Bandettini et al., 1993].

The images were filtered using a 3 × 3 median filter, which emphasized clusters of activation, and pixels below the corrected *P*-value of .05 were considered to be statistically reliable in individual subjects. These pixels were coregistered with the high-resolution anatomical scans for determination of the gross anatomy, and for presentation. Coregistration was achieved by applying linear translations and stretching of the functional images to match the anatomical images, after the statistical analyses had been performed. Quantification of significant activations was performed by counting the size of the activated cluster in each of five anatomically-defined regions, the calcarine cortex (inferior bank), lingual gyrus, posterior fusiform gyrus, inferior occipital gyrus, and middle occipital gyrus.

Electrophysiology

In the ERP recording session, EEG was recorded from 92 channels (.1–100 Hz bandpass), digitized at 256 Hz, and stored on hard disk for off-line analysis. Tin electrodes mounted in an elastic electrode cap (Electrocap International, Inc.) were used to record the EEG; electrode impedances were maintained below 5 KOhm. The electrodes were distributed across the scalp, and the precise 3-D locations were digitized for each subject, however, the topographic maps in Figure 1 were plotted using a single averaged electrode array applied to each subject's data. During recording, the scalp electrodes were referenced to the right mastoid process. Following artifact rejection for eye movements, blinks, blocking, and movement artifacts, ERPs were separately calculated for the nontarget and target bilateral arrays as a function of the differing task conditions (i.e., attend-left and attend-right). Only the data for the more frequent, nontarget stimuli are presented here, but the effects for target stimuli were very similar in the P1 time range. Scalp topographic mapping was performed using the spherical spline interpolation method of Perrin et al. [1989]. Repeated measures analysis of variance (ANOVA) was used to assess group statistical significance for the ERP data. The mean amplitude over the time window from 100 to 140 msec (P1 component) after stimulus onset was measured in each subject over occipital scalp sites. The well-established P1 attention effect would be reflected in an interaction of *direction of attention* (attend left vs. attend right) and *hemisphere of recording* (left hemisphere and right hemisphere).

RESULTS

Significant fMRI activations were found in each subject as the result of focused visual-spatial selective attention (Table I). When subjects attended the symbol pair in the left hemifield, the right posterior fusiform

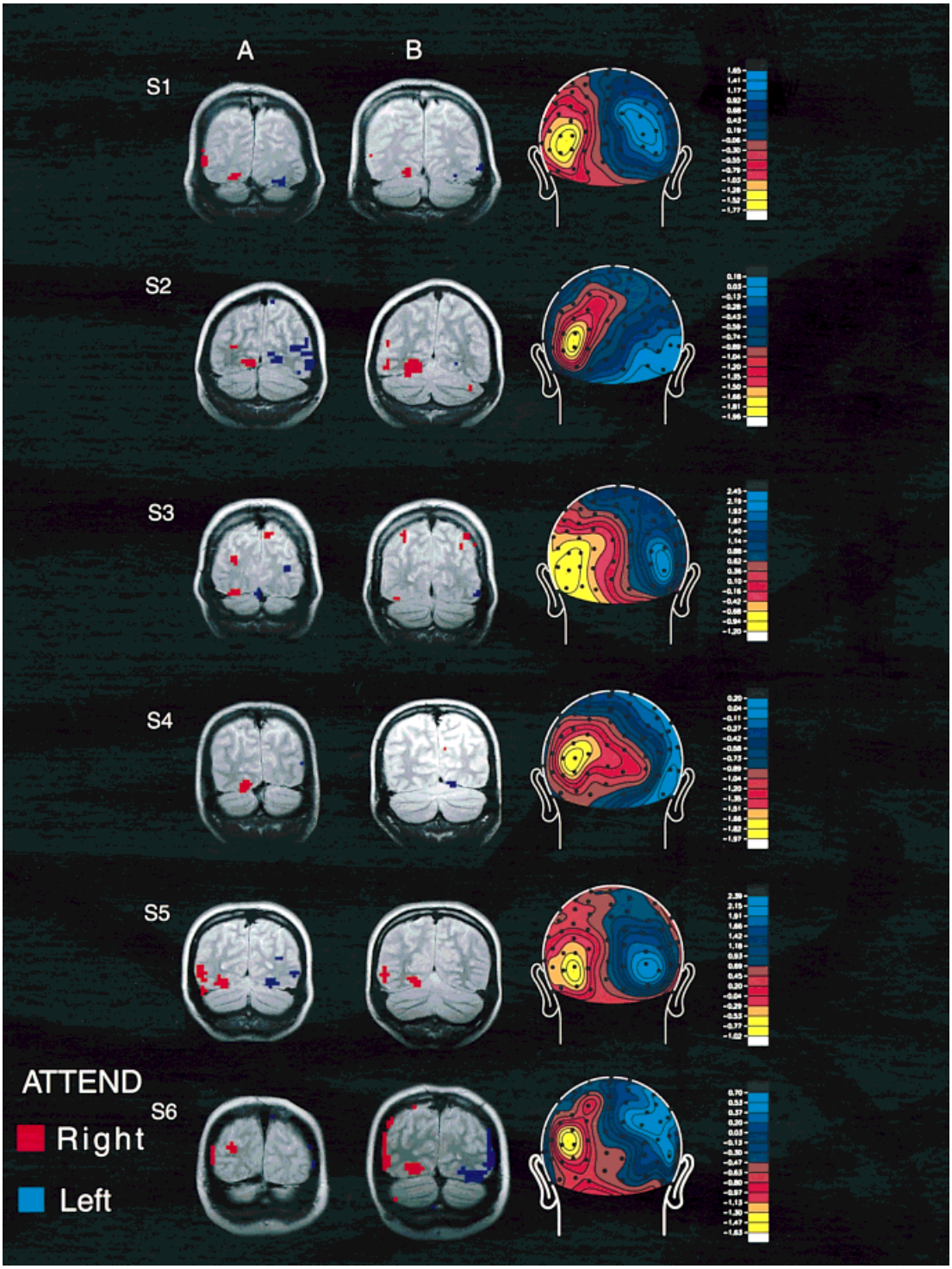

Figure 1.

Spatial attention effects in fMRI and ERP measures for each of the six subjects (S1–S6). Attention to the left half of the symbol arrays is shown in blue, and attention to the right in red in the fMRI images. The significantly activated pixels are overlaid onto high-resolution proton density scans from each subject. The topographic maps were computed from the mean voltage over the interval from 100–140 msec after stimulus onset, for the attend left minus attend right ERP waveforms, and are each autoscaled. As a result of the direction of the subtraction, in the topographic maps, the positive-going P1 attention effect over the left hemisphere for attend right appears as a negative polarity focus (red to yellow colors).

TABLE I. Activations in anatomically-defined regions of visual cortex contralateral to the direction of visual spatial attention (total over two slices of Fig. 1) size of cluster is in units of voxels

Subject	Anatomical region	Significant activation		Size of cluster	
		Left hemis	Right hemis	Left	Right
s1	Calcarine cortex	no	no	—	—
	Lingual gyrus	yes	no	7	—
	Posterior fusiform gyrus	yes	yes	7	11
	Inferior occipital gyrus	no	no	—	—
	Middle occipital gyrus	yes	yes	9	3
s2	Calcarine cortex	no	yes	—	3
	Lingual gyrus	yes	yes	9	3
	Posterior fusiform gyrus	yes	yes	17	4
	Inferior occipital gyrus	yes	yes	7	5
	Middle occipital gyrus	yes	yes	3	28
s3	Calcarine cortex	no	no	—	—
	Lingual gyrus	no	yes	—	4
	Posterior fusiform gyrus	yes	no	5	—
	Inferior occipital gyrus	yes	yes	4	3
	Middle occipital gyrus	no	yes	—	4
s4	Calcarine cortex	no	no	—	—
	Lingual gyrus	yes	no	4	—
	Posterior fusiform gyrus	yes	yes	7	5
	Inferior occipital gyrus	no	no	—	—
	Middle occipital gyrus	no	yes	—	1
s5	Calcarine cortex	no	no	—	—
	Lingual gyrus	no	no	—	—
	Posterior fusiform gyrus	yes	yes	18	8
	Inferior occipital gyrus	yes	no	3	—
	Middle occipital gyrus	yes	yes	18	4
s6	Calcarine cortex	no	no	—	—
	Lingual gyrus	yes	no	4	—
	Posterior fusiform gyrus	yes	yes	6	12
	Inferior occipital gyrus	yes	yes	3	10
	Middle occipital gyrus	yes	yes	8	16

gyrus showed increased blood flow, and when attention was directed to the right, this activation was found in the left posterior fusiform gyrus. These effects are shown for each subject mapped onto high-resolution anatomical scans in Figure 1.

The two adjacent coronal sections for each subject were taken through the occipital lobe at the level of the posterior fusiform gyrus. In the figure, blue colored pixels indicate those that are correlated with attending to the left, and red colored with attending to the right. The right hemisphere is on the right of each figure. These data show that attention-related activations were relatively consistent across subjects. All subjects showed contralateral posterior fusiform activation for spatial attention, with the exception of subject 3 (S3), for whom no activation reached significance at the .05 level in the right hemisphere for the filtered data considered here.

In addition to the activations in the fusiform gyrus, there was also evidence of activations in other areas of extrastriate visual cortex, such as the middle occipital gyrus. The middle occipital gyrus activations were similar to those we have reported previously using PET in that the pattern showed an increase in blood flow in the hemisphere contralateral to the attended hemifield [c.f., Mangun et al., 1997].

Activations in lingual and inferior occipital gyri were also observed in some subjects. Sporadic activations were observed in the parietal cortex, but these were not as robust or consistent across subjects. For

example, in subjects 3 and 6, activations were observed in inferior parietal lobe during attention to the right hemifield.

The ERPs also showed significant amplitude modulations ($P < .05$ for interaction of *direction of attention* and *hemisphere of recording* across the six subjects) in the P1 latency range, that we refer to as the P1 attention effect. These effects reflected the fact that the P1 was more positive in amplitude over the occipital scalp regions contralateral to the attended hemifield. These are shown for each subjects as topographic voltage maps computed for the period from 100–140 msec after the onset of the nontarget bilateral symbol arrays (Fig. 1). As can be observed in the figure, each subject showed a contralateral occipital attentional focus on the scalp that corresponds to the P1 attention effect. These foci of attentional modulations were highly consistent over the left hemisphere (six out of six subjects), but were more variable over the right hemisphere. Only group statistics were calculated for the ERPs.

DISCUSSION

These data clearly demonstrate focal attention-related activity as measured by fMRI in single subjects. The pattern of results provides a clear replication of our prior findings of activations in the contralateral fusiform gyrus, and middle occipital gyrus with spatial attention. Moreover, these data indicate that activations in the posterior fusiform and middle occipital gyri are relatively consistent across subjects, as would be predicted by our prior PET results [Heinze et al., 1994; Mangun et al., 1997; see also O'Leary et al., 1997]. In addition, in some subjects, activations in the more medially located lingual gyrus, and ventral lateral inferior occipital gyrus were also observed. These activations were less consistent across subjects and would explain why they might not have been observed in our prior PET studies which relied on group averaged data.

Attentional modulations of the occipital P1 component were observed in all subjects, and thus are in line with numerous previous studies of spatial attention [e.g., Eason, 1981; Van Voorhis and Hillyard, 1977; Mangun and Hillyard, 1991; Mangun et al., 1993]. However, the scalp distribution of the P1 effects were somewhat variable across subjects. This is most likely due to differences in the underlying 3-D anatomy of the neural generators of the P1 effect. The scalp distribution of ERPs is influenced strongly by the orientation of the underlying neural generators [e.g., Nunez, 1981]. Hence, across subjects a relatively large variation in scalp distribution can be produced by neurons located in equivalent anatomical loci, due merely to changes in the orientation of the local cortical surface with respect to the scalp recording sites. In all subjects, however, a positive polarity ERP attention effect was clearly observed over the contralateral occipital scalp in the P1 latency range.

These data can be interpreted in light of our general model of visual-spatial selective attention [see Mangun, 1995]. When subjects attend to regions of visual space, incoming signals processed in visual extrastriate cortex are modulated. The activations in contralateral fusiform gyrus most probably represent increased neural processing for the stimuli presented in the selected region of space. These data in humans fits well with an ever growing body of evidence from single unit recordings in monkeys that has demonstrated that spatial attention can influence neuronal firing rates in various extrastriate areas [e.g., Moran and Desimone, 1985; Motter, 1994].

Some data from work in monkeys [Motter, 1993] suggests that the striate cortex might also be modulated during spatial selective attention. There has also been a recent fMRI report that nonselective attention to motion (attending vs. passive viewing) results in changes in V1 activity [Watanabe et al., 1998]. However, in the present study, no compelling evidence for activations in striate cortex were observed. It is important to note, however, that the present analyses related functional activations to gross anatomical regions of visual cortex, not to functionally-defined areas as is possible to do using fMRI [Engel et al., 1994; Sereno et al., 1995]. Thus, a clear conclusion as to the relationship between some of the present activations in ventral-medial areas (lingual gyrus) and the borders of striate cortex cannot be drawn [however, see Mangun et al., 1998b). In general, though, activations in the calcarine region were not observed (except in one hemisphere in one subject, S2). Given the emphasis on clustered activity in the present analyses, it is possible that small activations in the calcarine region may have been overlooked. Alternatively, it may be that during selective spatial attention where competing stimuli are widely separated, that the striate cortex is not engaged to achieve selective processing of visual inputs.

Importantly for progress in integration of electromagnetic and functional neuroimaging data [e.g., Mangun et al., 1998a], the present results underscore both the consistency of ERP and fMRI measures of neural processing, as well as the variability between subjects. The latter is especially true for the scalp-recorded ERPs, due to the sensitivity of the scalp-recorded signal to the orientation of the intracranial neuronal

generators. Future work should take into account this intersubject variability in order to improve the resolution of integrated modeling. The intersubject variability in anatomy and functional anatomy should not be thought of as limiting the prospects for multimethodological integration. Rather, the unique functional neural architecture of individuals can serve as a source of information to be used to achieve higher-resolution views of human brain function.

ACKNOWLEDGMENTS

We thank Dr. Joseph Dien for helpful comments, Valerie Clark for assistance with Figure 1, and Dan Deal for technical assistance. We are grateful to the volunteers who participated in this study. This research was supported by grants from the Human Frontiers Science Program Organization, the NIMH, and the NINDS.

REFERENCES

Bandettini PA, Jesmanowicz A, Wong EC, Hyde, JS (1993): Processing strategies for time-course data sets in functional MRI of the human brain. Magn Reson Med 30:161–173.

Buonocore MH, Gao L (1997): Ghost artifact reduction for echo-planar imaging using image phase correction. Magn Reson Med 38:89–100.

Buonocore MH, Maddock RJ (1997): Noise suppression digital filters for functional MRI using image reference data. Magn Reson Med 38:456–469.

Corbetta M, Miezin FM, Dobmeyer S, Shulman GL, Petersen SE (1991): Selective and divided attention during visual discriminations of shape, color, and speed: Functional anatomy by positron emission tomography. J Neurosci 11:2383–2402.

Dale A, Sereno M (1993): Improved localization of cortical activity by combining EEG and MEG with MRI cortical surface reconstruction: A linear approach. J Cogn Neurosci 5:162–176.

Eason RG (1981): Visual evoked potential correlates of early neural filtering during selective attention. Bull Psychonom Soc 18:203–206.

Engel SA, Rumelhart DE, Wandell BA, Lee AT, Glover GH, Chichilinsky EJ, Shadlen MN (1994): fMRI of human visual cortex. Nature 370:106.

Heinze HJ, Mangun GR, Burchert W, Hinrichs H, Scholz M, Münte TF, Gös A, Johannes S, Scherg M, Hundeshagen H, Gazzaniga MS, Hillyard SA (1994): Combined spatial and temporal imaging of spatial selective attention in humans. Nature 392:543–546.

Kwong K, Belliveau J, Chesler D, Goldberg J, Weisskoff R, Poncelet B, Kennedy D, Hoppel B, Cohen M, Turner R, Cheng H, Brady T, Rosen B (1992): Dynamic magnetic resonance imaging of human brain activity during primary sensory stimulation. Proc Natl Acad Sci USA 89:5675–5679.

Luck SJ, Hillyard SA, Mouloua M, Woldorff MG, Clark VP, Hawkins HL (1994): Effects of spatial cuing on luminance detectability: Psychophysical and electrophysiological evidence for early selection. J Exp Psychol: Hum Percep Perf 20:887–904.

Mangun GR (1995): Neural mechanisms of visual selective attention in humans. Psychophysiology 32:4–18.

Mangun GR, Hillyard SA (1991): Modulation of sensory-evoked brain potentials provide evidence for changes in perceptual processing during visual-spatial priming. J Exp Psych: Hum Percep Perf 17:1057–1074.

Mangun GR, Hillyard SA, Luck SJ (1993): Electrocortical substrates of visual selective attention. In: Meyer D, Kornblum S (eds): Attention and Performance XIV. Cambridge, MA: MIT Press, pp 219–243.

Mangun GR, Hopfinger J, Kussmaul C, Fletcher E, Heinze HJ (1997): Covariations in PET and ERP measures of spatial selective attention in human extrastriate visual cortex. Hum Brain Mapp 5:273—279.

Mangun GR, Hopfinger J, Heinze HJ (1998a): Integrating functional neuroimaging and electromagnetic recording in the study of human cognition. Behav Res Method, Instrum Comput 30:118–130.

Mangun GR, Buonocore M, Girelli M, Jha A (1998b): Early spatial attention gates information in multiple functionally-defined visual areas: An fMRI and ERP study in humans. Neuroimage 7:S71.

Moran J, Desimone R (1985): Selective attention gates visual processing in the extrastriate cortex. Science 229:782–784.

Motter BC (1993): Focal attention produces spatial selective processing in visual cortical areas V1, V2 and V4 in the presence of competing stimuli. J Neurophysiol 70:909–919.

Motter BC (1994): Neural correlates of attentive selection for color or luminance in extrastriate area V4. J Neurosci 14:2178–189.

Nunez P (1981): Electric Fields of the Brain. New York: Oxford University Press.

Ogawa S, Tank D, Menon R, Ellerman J, Kim S, Merkle H, Urgibil K (1992): Intrinsic signal changes accompany sensory stimulation: Functional brain mapping with magnetic resonance imaging. Proc Natl Acad Sci USA 89:5951–5955.

OLeary DS, Andreasen NC, Hurtig RR, Torres IJ, Flashman LA, Kesler ML, Arndt SV, Cizaldo TJ, Ponto LL, Watkins GL (1997): Auditory and visual attention assessed with PET. Hum Brain Mapp 5:422–436.

Perrin F, Pernier J, Bertrand O, Echallier J (1989): Spherical splines for scalp potential and current density mapping. Electroencephalography Clin Neurophysiol 72:184–187.

Sereno MI, Dale AM, Reppas JB, Kwong KK, Belliveau JW, Brady TJ, Rosen BR, Tootell RB (1995): Borders of multiple visual areas in humans revealed by functional magnetic resonance imaging. Science 268:889–893.

Van Voorhis ST, Hillyard SA (1977): Visual evoked potentials and selective attention to points in space. Percep Psychophysics 22:54–62.

Watanabe T, Sasaki Y, Miyauchi S, Putz B, Fujimaki N, Nielsen M, Takino R, Miyakawa S (1998): Attention-regulated activity in human primary visual cortex. J Neurophysiol 79:2218–2221.

Woldorff M, Fox P, Matzke M, Lancaster J, Veeraswamy J, Zamarripa F, Seabolt M, Glass T, Gao J, Martin C, Jerabek P (1997): Retinotopic organization of the early visual spatial attention effects as revealed by PET and ERPs. Hum Brain Mapp 5:280–286.